Catalysis of Carbamate Hydrolysis by Vancomycin and Semisynthetic Derivatives

Zheng Shi and John H. Griffin*

Contribution from the Department of Chemistry, Stanford University, Stanford, California 94305-5080

Received May 29, 1992

Abstract: The semisynthesis of vancomycin (**1a**) derivatives bearing propyl (**1b**), histaminyl (**1c**), and 3-aminopropyl (**1d**) groups attached to the C-terminus is reported. This work was undertaken as part of a program to create new biomimetic catalysts and to ultimately test the relative potencies of antibiotics that act stoichiometrically versus catalytically against a common target. **1b-d** were prepared by dicyclohexylcarbodiimide-mediated condensations between vancomycin's carboxyl group and amine coupling partners and were found to bind to N^{α},N^{ω}-diacetyl-L-Lys-D-Ala-D-Ala (**2a**, a tripeptide analogue of the C-terminus of the *Staphylococcus aureus* cell wall precursor) with affinities similar to that observed with **1a**. **1a-d** exhibit novel carbamate hydrolase activity, catalyzing the hydrolysis of N^{α}-(*p*-nitrophenyloxycarbonyl-Gly)-N^{ω}-acetyl-L-Lys-D-Ala-D-Ala (**2b**) with demonstrated substrate turnover, specificity, and inhibition by **2a**. Catalytic rate constants (k_{cat}) for hydrolysis of **2b** were 0.55, 0.97, 1.14, and 1.48 min^{-1} for **1a-d**, respectively. These rate constants correspond to accelerations of 4–11-fold above the buffer-catalyzed reaction (k_{cat}/k'_{buf}) and 2200–5900-fold above the uncatalyzed reaction (k_{cat}/k'_{uncat}) with effective molarities (k_{cat}/k_{buf}) of 0.085–0.23 M. Differences in k_{cat} among the series **1a-d** were small and did not correlate with the presence or absence of C-terminal catalytic functional groups. The variation in rate constants did correlate with increases in positive charge at the C-terminus of **1a-d**. The microenvironment in the region where hydrolysis occurs was probed using the ligand N^{α}-(fluoresceinylthiocarbamoyl)-N^{ω}-acetyl-L-Lys-D-Ala-D-Ala (**2c**), which has a pH-dependent absorption spectrum. The spectral changes observed upon complexation of **2c** to **1a-d** were consistent with an increase in microscopic pH and/or a decrease in pK_a in this region relative to the bulk solution. Trends in $\Delta pH/\Delta pK_a$ correlate with the trend in k_{cat} for **1a-d** although the apparent increase in microscopic hydroxide ion concentration could not quantitatively account for the observed rate accelerations above the buffer-catalyzed reaction.

Vancomycin (**1a**, Figure 1) is the prototype of the glycopeptide family of antibacterial agents. These antibiotics bind to the C-terminus of peptidoglycan precursors and prevent their incorporation into the polymeric bacterial cell wall.[1] The novel receptorlike mode of action of vancomycin-class antibiotics and their clinical efficacy[2] have inspired studies of their structures and the structures of their complexes with peptidoglycan precursors,[3] their semisynthetic modification,[4] their total synthesis,[5] and their use as paradigms for molecular recognition.[6] We have initiated a research program directed at the design and preparation of vancomycin derivatives capable of catalyzing chemical reactions, including the cleavage of peptidoglycan precursors. Such molecules are of interest as enzyme mimetics and as a framework within which to test the relative potencies of antibiotics that act stoichiometrically versus catalytically against a common target. In this paper, we report that vancomycin and semisynthetic derivatives bearing propyl, imidazole, and amino groups tethered to the C-terminus via amide bonds catalyze the hydrolysis of a *p*-nitrophenyloxycarbamate linkage attached to a peptidoglycan precursor fragment and that the observed rate accelerations correlate with increases in positive charge and changes in the microenvironment in the region where hydrolysis occurs.

(1) Perkins, H. R.; Nieto, M. *Pure Appl. Chem.* **1973**, *35*, 371–381.
(2) Wise, R., Reeves, D., Eds. *J. Antimicrob. Chemother.* **1984**, *14*, Supplement D.
(3) (a) Sheldrick, G. M.; Jones, P. G.; Kennard, O.; Williams, D. H.; Smith, G. A. *Nature* **1978**, *271*, 223–225. (b) Harris, C. M.; Harris, T. M. *J. Am. Chem. Soc.* **1982**, *104*, 4293–4295. (c) Williams, D. H.; Rajanada, V.; Williamson, M. P.; Bojesen, G. *Top. Antibiot. Chem.* **1980**, *5B*, 119–158. (d) Fesik, S. W.; O'Donnell, T. J.; Gampe, R. T., Jr.; Olejniczak, E. T. *J. Am. Chem. Soc.* **1986**, *108*, 3165. (e) Molinari, H.; Pastore, A.; Lian, L.; Hawkes, G. E.; Sales, K. *Biochemistry* **1990**, *29*, 2271–2277. (f) Popieniek, P. H.; Pratt, R. F. *J. Am. Chem. Soc.* **1991**, *113*, 2264–2270.
(4) (a) Malabarba, A.; Trani, A.; Ferrari, P.; Pallanza, R.; Cavalleri, B. *J. Antiobiot.* **1987**, *40*, 1572–1587. (b) Malabarba, A.; Trani, A.; Strazzolini, P.; Cietto, G.; Ferrari, P.; Tarzia, G.; Pallanza, R.; Berti, M. *J. Med. Chem.* **1989**, *32*, 2450–2460. (c) Trani, A.; Malabarba, A.; Ferrari, P.; Pallanza, R. *J. Antibiot.* **1990**, *43*, 1471–1482. (d) Nagarajan, R.; Schabel, A. A.; Occolowitz, J. L.; Counter, F. T.; Ott, J. L. *J. Antibiot.* **1988**, *41*, 1430–1438. (e) Nagarajan, R.; Schabel, A. A.; Occolowitz, J. L.; Counter, F. T.; Ott, J. L.; Felty-Duckworth, A. M. *J. Antibiot.* **1989**, *42*, 63–72.
(5) Evans, D. A.; Ellman, J. A.; DeVries, K. M. *J. Am. Chem. Soc.* **1989**, *111*, 8912–8914.
(6) (a) Williams, D. H.; Cox, J. P. L.; Doig, A. J.; Gardner, M.; Gerhard, U.; Kaye, P. T.; Lal, A. R.; Nicholls, I. A.; Salter, C. J.; Mitchell, R. C. *J. Am. Chem. Soc.* **1991**, *113*, 7020–7030. (b) Hobbs, D. W.; Still, W. C. *Tetrahedron Lett.* **1987**, *28*, 2805–2808. (c) Hong, J.-I.; Namgoong, S. K.; Bernardi, A.; Still, W. C. *J. Am. Chem. Soc.* **1991**, *113*, 5111–5112. (d) Pant, N.; Hamilton, A. D. *J. Am. Chem. Soc.* **1988**, *110*, 2002–2003.

Results

Design and Semisynthesis. We chose to modify the C-terminus of vancomycin for three reasons. First, the NMR-determined structures of glycopeptide:peptide complexes[3] and CPK models indicate that groups tethered to the C-terminus may interact with bound peptidoglycan precursors. Second, it has been shown that esters, carboxamides, and carboxyhydrazides of the glycopeptide antibiotic teicoplanin retain peptide-binding and antibacterial activities.[4a-c] Third, we expected that vancomycin's sole carboxylate could be selectively activated and coupled with amines to form amides. We chose to add the imidazole functional group on the basis of the catalytic roles it plays in enzymes[7] and antibodies[8a-d] that catalyze acyl-transfer reactions, and the amino functional group for its potential to act as a nucleophile or general base (when unprotonated) or to stabilize anionic transition states or serve as a general acid (when protonated).[7]

Vancomycin propanamide (**1b**), vancomycin histamide (**1c**), and vancomycin 3-aminopropanamide (**1d**) were prepared by

(7) Walsh, C. *Enzymatic Reaction Mechanisms*; W. H. Freeman: San Francisco, CA, **1979**; pp 49–107.
(8) (a) Tramontano, A.; Janda, K. D.; Lerner, R. A. *Science* **1986**, *234*, 1566–1570. (b) Pollack, S. J.; Schultz, P. G. *J. Am. Chem. Soc.* **1989**, *111*, 1929–1931. (c) Baldwin, E.; Schultz, P. G. *Science* **1989**, *245*, 1104–1107. (d) Jackson, D. Y.; Prudent, J. R.; Baldwin, E. P.; Schultz, P. G. *Proc. Natl. Acad. Sci. U.S.A.* **1991**, *88*, 58–62. (e) Green, B. S.; Eshar, Z.; Tawfik, D. S.; Zemel, R. R.; Arad-Yellin, R. *Biochemistry* **1990**, *29*, 9916–9921.

0002-7863/93/1515-6482$04.00/0

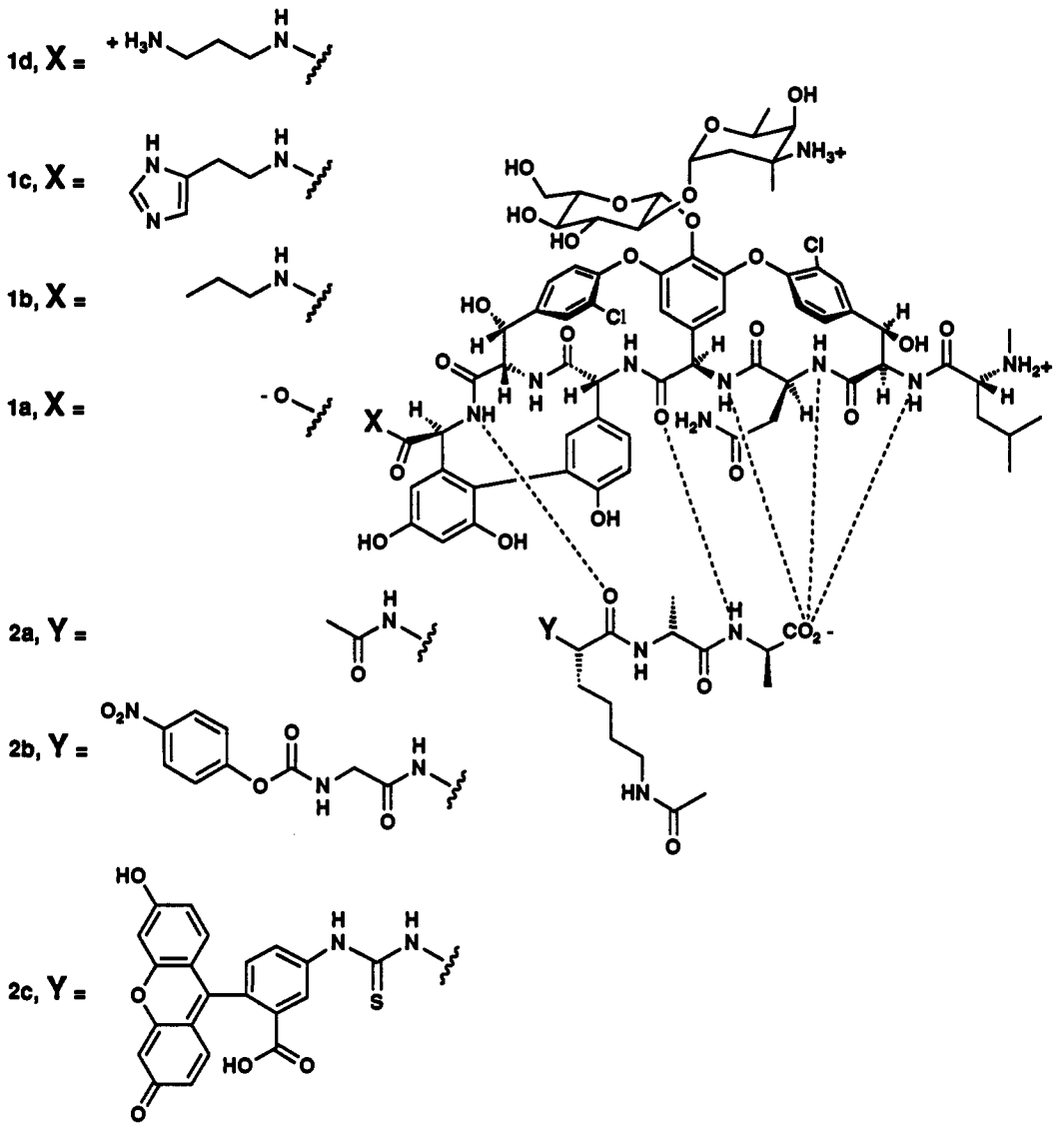

Figure 1. Model of complexes formed between vancomycin (**1a**), vancomycin propanamide (**1b**), vancomycin histamide (**1c**), and vancomycin 3-aminopropanamide (**1d**) with N^{α},N^{ω}-diacetyl-L-Lys-D-Ala-D-Ala (**2a**), N^{α}-(*p*-nitrophenyloxycarbonyl-Gly)-N^{ω}-acetyl-L-Lys-D-Ala-D-Ala (**2b**), and N^{α}-(fluoresceinylthiocarbamoyl)-N^{ω}-acetyl-L-Lys-D-Ala-D-Ala (**2c**). The peptides are bound within the cleft of vancomycin via specific hydrogen bonds (dashed lines) and van der Waals contacts.[3]

coupling vancomycin with 1-aminopropane, histamine, and 1,3-diaminopropane, respectively. Coupling reactions were mediated by the combination of dicyclohexylcarbodiimide and *N*-hydroxybenzotriazole and were carried out in dimethyl sulfoxide solvent. A 5–10-fold excess of each amine was used to minimize vancomycin self-coupling. The products were purified by reverse-phase HPLC and characterized by high-field ^{1}H NMR and LSIMS. The ^{1}H NMR spectra exhibited resonances expected for vancomycin, the appendages, and new amide NHs. The LSIMS exhibited the expected parent ions as well as ions which corresponded to loss of methylamine, vancosamine, and vancosamine plus glucose.

Peptide Ligands and Substrates. The tripeptide N^{α},N^{ω}-diacetyl-L-Lys-D-Ala-D-Ala (**2a**) mimics the C-terminus of the peptidoglycan precursor from *Staphylococcus aureus* and represents the best known ligand for vancomycin.[9] N^{α}-(*p*-Nitrophenyloxycarbonyl-Gly)-N^{ω}-acetyl-L-Lys-D-Ala-D-Ala (**2b**) and N^{α}-(fluoresceinylthiocarbamoyl)-N^{ω}-acetyl-L-Lys-D-Ala-D-Ala (**2c**) bear a hydrolyzable carbamate linkage and a pH-sensitive dye at their respective N-termini. Models indicate that these groups will lie in proximity to the C-terminus of **1a-d** upon glycopeptide:peptide association. **2a,b** were synthesized in their entirety by stepwise solid-phase synthesis. **2c** was prepared by reaction of N^{ω}-acetyl-L-Lys-D-Ala-D-Ala (an intermediate in the solid-phase synthesis of **2a**) with fluorescein isothiocyanate in solution. **2a-c** were purified by reverse-phase HPLC and characterized by high-field ^{1}H NMR and LSIMS.

Binding Studies. Affinities of vancomycin and the semisynthetic derivatives **1b-d** for **2a** were determined using difference UV spectroscopy.[9] The apparent dissociation constants (K_d) for the **1a-d**:**2a** complexes were similar, ranging from 0.64 to 1.0 μM (Table I). Thus, addition of propyl, histaminyl, or 3-aminopropyl groups to vancomycin via formation of amide bonds at the C-terminus has little effect on peptide-binding affinity.

Catalysis of Carbamate Hydrolysis. Hydrolytic activities of **1a-d** were assayed using the chromogenic substrate **2b**. Reactions were carried out at 25 °C in 20 mM sodium phosphate buffer (pH 7.0) and were monitored by measuring the increase in absorbance at 400 nm due to the formation of *p*-nitrophenolate anion. HPLC was used to confirm the identity of hydrolysis products *p*-nitrophenol and Gly-N^{ω}-acetyl-L-Lys-D-Ala-D-Ala. Under these conditions, the pseudo-first-order rate constant for buffer-catalyzed hydrolysis of **2b** ($k'_{buf} = k_{buf}$[buffer]) was

(9) (a) Nieto, M.; Perkins, H. R. *Biochem. J.* **1971**, *123*, 773–787. (b) Nieto, M.; Perkins, H. R. *Biochem. J.* **1971**, *123*, 789–803. (c) Kannan, R.; Harris, C. M.; Harris, T. M.; Waltho, J. P.; Skelton, N. J.; Williams, D. H. *J. Am. Chem. Soc.* **1988**, *110*, 2946–2953.

Table I. Rate Constants and Microscopic pH Data for Vancomycin and Semisynthetic Derivatives

catalyst	K_d (μM)	k_{cat} (min^{-1})	accel (k_{cat}/k'_{buf})[a]	accel (k_{cat}/k'_{uncat})[b]	EM[c] (M) (k_{cat}/k_{buf})	pH_m[d]
none		0.000 25[e]		1.0		
buffer		0.13 ± 0.01[f]	1.0	520	0.020	
1a	0.67 ± 0.1	0.55 ± 0.04	4.2	2200	0.085	7.14
1b	1.0 ± 0.4	0.97 ± 0.03	7.5	3900	0.15	7.17
1c	0.70 ± 0.2	1.14 ± 0.02	8.8	4600	0.18	7.21
1d	0.64 ± 0.2	1.48 ± 0.03	11	5900	0.23	7.24

[a] Rate acceleration over buffer-catalyzed reaction. [b] Rate acceleration over uncatalyzed reaction. [c] Effective molarity. [d] Spectroscopically determined apparent microscopic pH at the C-terminus of **1a–d**:**2c** complexes in bulk solution pH of 7.0. [e] Pseudo-first-order rate constant for hydrolysis of **2b** in water at pH 7.0. [f] Pseudo-first-order rate constant for hydrolysis of **2b** in 20 mM sodium phosphate buffer, pH 7.0 ($k'_{buf} = k_{buf}$[buffer]).

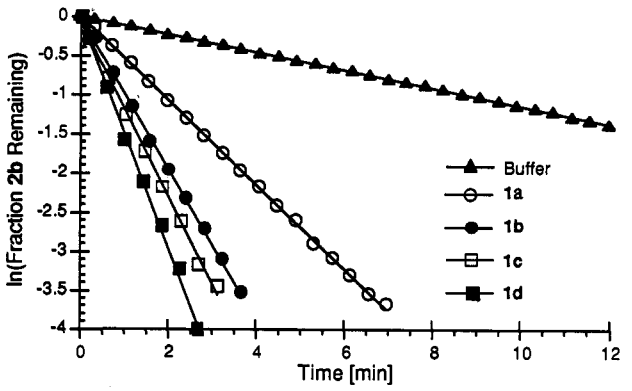

Figure 2. Representative kinetic data for hydrolysis of **2b** by 20 mM sodium phosphate buffer (pH 7.0) (filled triangles), **1a** (circles), **1b** (filled circles), **1c** (boxes), and **1d** (filled boxes). Concentrations: **1a–d**, 91–96 μM; **2b**, 25–60 μM.

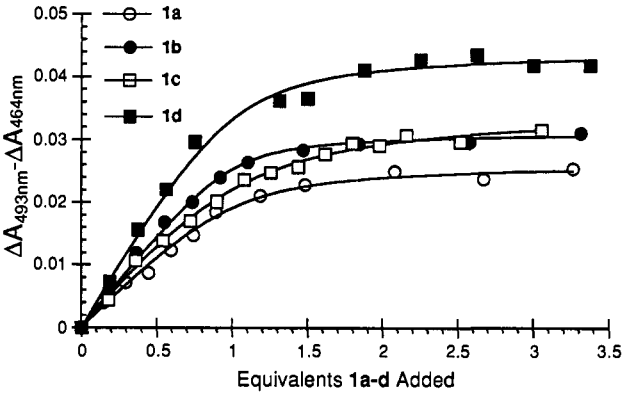

Figure 3. Changes in absorbance observed upon addition of **1a** (circles), **1b** (filled circles), **1c** (boxes), and **1d** (filled boxes) to **2c** (6.4 μM).

determined to be 0.13 min^{-1}, indicating $k_{buf} = 6.5$ M^{-1} min^{-1}. The rate of buffer-catalyzed hydrolysis was found to increase linearly with the hydroxide ion concentration within the pH range 5.5–7.5. The pseudo-first-order rate constant for hydrolysis of **2b** in pure water at pH 7.0 (k'_{uncat}) was estimated to be 2.5×10^{-4} min^{-1} by measuring k'_{buf} at a series of buffer concentrations (0.5–20 mM) and extrapolating to zero buffer concentration.

Addition of vancomycin or the derivatives **1b–d** to the buffer significantly accelerated the rate of hydrolysis of **2b**. The limited sensitivity of the experimental assay and interference from buffer-catalyzed hydrolysis precluded a classical steady-state kinetic treatment of these reactions, which would have required the use of concentrations of **1a-d** well below K_d and concentrations of **2b** spanning K_d, the expected K_m. Rate constants (k_{cat}) for hydrolysis were obtained through analysis of reactions in which **1a-d** were in excess of **2b** and in which **2b** was used at concentrations higher than the measured K_d values. Under these conditions, it could be assumed that **2b** was fully bound to **1a-d** and that background hydrolysis could be neglected. Plots of ln(fraction **2b** remaining) versus time were linear through at least four half-lives (Figure 2). Hydrolysis rates were found to be linearly dependent on the concentration of **2b** and independent of the concentration of **1a-d** provided **1a-d** were present in excess. Values for k_{cat} ranged from 0.55 min^{-1} for **1a** to 1.48 min^{-1} for **1d**. These rate constants correspond to rate accelerations of 4–11-fold above the buffer-catalyzed reaction (k_{cat}/k'_{buf}), 2200–5900-fold above the uncatalyzed reaction (k_{cat}/k'_{uncat}), and reflect effective molarities (k_{cat}/k_{buf}) of 0.085–0.23 M (Table I).

Substrate turnover was demonstrated in reactions carried out using **2b** in excess of **1a-d** after correcting for buffer-catalyzed hydrolysis of the unbound substrate. It was also determined that hydrolysis of **2b** by **1a-d** was inhibited by **2a**, that **1a-d** did not accelerate the hydrolysis of the noncognate substrate *p*-nitrophenyloxycarbamoyl-β-alanine methyl ester, and that replacing **1a-d** with similar concentrations of sodium acetate and/or imidazole did not accelerate the hydrolysis of **2b** significantly above the buffer-catalyzed background rate. These findings support the notion that acceleration of the rate of carbamate hydrolysis by **1a-d** involves substrate binding.

Probe of Microenvironment. The microenvironment in the region where carbamate hydrolysis occurs within **1a-d**:**2b** complexes was probed using the fluoresceinylated tripeptide ligand **2c**, which has a pH-dependent absorption spectrum. The extinction coefficients of **2c** at 493 and 464 nm increase and remain constant with increases in pH, respectively. It was found that differences in adsorption at 493 versus 464 nm increased upon addition of **1a-d** to **2c** (Figure 3). These results are consistent with an increase in microscopic pH near the C-terminus of **1a-d** in their complexes with peptides, with a decrease in the pK_a of **2c** upon binding to **1a-d**, or with a combination of these phenomena. To simplify quantitative consideration of the spectral changes, the data are interpreted in what follows as apparent increases in microscopic pH. By measuring the maximum change in the differences of absorption at 493 and 464 nm upon addition of **1a-d** to **2c** and comparing these changes to a standard curve derived from absorption spectra of **2e** at a series of pH values, it was possible to provide a measure of the apparent microscopic pH experienced by the carbamate group of **2b** when it is bound to **1a-d**. These ranged from pH 7.14 with vancomycin to 7.24 with **1d** (Table I). Increases in apparent microscopic pH correlated with increased positive charge on the C-terminal functional groups of **1a-d** and with k_{cat}. The absorption spectra of noncognate probes (fluorescein isothiocyanate, fluoresceinylthiocarbamoyl-β-alanine methyl ester) were found to be unperturbed by addition of **1a-d**. The spectroscopic titration data were also analyzed to afford apparent dissociation constants for the **1a-d**:**2c** complexes. K_d's obtained by this method were 0.67 ± 0.03 for **1a**:**2c**, 0.33 ± 0.04 for **1b**:**2c**, 1.3 ± 0.1 for **1c**:**2c**, and 0.65 ± 0.1 μM for **1d**:**2c**.

Discussion

The dicyclohexylcarbodiimide-mediated coupling of vancomycin with amines constitutes a simple and selective method for the semisynthesis of vancomycin derivatives bearing alkyl, imidazole, and amine functional groups attached to the C-terminus. The method does not require any protection of vancomycin

and should be applicable to the preparation of derivatives bearing different functional groups and/or tethers. Derivatives **1b-d** bind to the peptidoglycan precursor fragment **2a** with affinities similar to that observed with vancomycin, indicating that the appended groups of **1b-d** either interact little with the bound peptide or engage in stabilizing and destabilizing interactions of similar magnitude.

The naturally occurring antibiotic vancomycin and the semisynthetic derivatives **1b-d** exhibit novel and specific carbamate hydrolase activity. **1a-d** catalyze the hydrolysis of substrate **2b** at rates which are 4–11-fold higher than the buffer-catalyzed reaction. Relative to the uncatalyzed reaction in water, combinations of **1a-d** and buffer afford rate accelerations of 2200–5900-fold.[10] These rate accelerations are similar to those obtained with antibodies[8] and model systems[11] that catalyze analogous acyl-transfer reactions, but are far below the rate enhancements observed with enzymes that catalyze the hydrolysis of *p*-nitrophenyl anilides.[12]

While the catalytic rate constants for hydrolysis of **2b** vary among the series **1a-d**, differences in k_{cat} are small and there is no obvious correlation between the identity of the C-terminal functional groups of **1a-d** and k_{cat}. Indeed the k_{cat} for **1b**, which bears a C-terminal alkyl appendage, is greater than that for **1a**, which bears a potentially catalytic carboxyl group. These results prompted us to examine whether more general microenvironmental effects may be operating in these systems. We probed the region of **1a-d**:**2b** complexes where carbamate hydrolysis occurs using the pH-sensitive chromophoric ligand **2c** and in each case observed spectral changes that were consistent with increases in microscopic pH and/or decreases in carboxyl pK_a relative to the bulk solution. These two effects (ΔpH versus ΔpK_a) cannot be distinguished by the data, but both indicate that negatively charged species (hydroxide ions, carboxylate ions, and anionic transition states) will be attracted to and/or stabilized in the region where carbamate hydrolysis occurs.

The trends in $\Delta pH/\Delta pK_a$ within the series **1a-d** correlate with increased positive charge at the C-terminus (carboxylate < alkyl < imidazole/imidazolium < ammonium). Increased positive charge would be expected to increase attraction for hydroxide anions and stabilization of anions. It is not known why vancomycin, which possesses a C-terminal carboxylate, exhibits a microenvironment favorable for the attraction or formation of additional anions. The pK_a of the vancomycin carboxyl (2.9)[9a] is lower than is generally observed for the C-terminal carboxyl groups of peptides, indicating that the structure of vancomycin favors the formation of the carboxylate ion. Studies of vancomycin derivatives modified at other positions and calculation of the electrostatic forces exerted on anions which surround the complex between vancomycin and a peptidoglycan precursor fragment may provide further understanding of this effect.

The trends in $\Delta pH/\Delta pK_a$ also correlate with the trend in k_{cat} for **1a-d**. This is consistent with a model in which binding of **2b** to **1a-d** brings the *p*-nitrophenyloxycarbamoyl group into a region of increased hydroxide ion concentration and/or increased anion stability, where its hydrolysis is accelerated. If the observed spectral changes are interpreted solely in terms of a ΔpH phenomenon, apparent increases in microscopic pH of 0.14–0.24 units indicate increases in microscopic hydroxide ion concentration of 1.38–1.74-fold. These do not quantitatively account for the observed 4–11-fold rate accelerations above the buffer-catalyzed reaction. It is possible that the increase in microscopic pH experienced by the carbonyl group of **2b** may be underestimated by spectral titrations with **2c**. Increases in local hydroxide ion concentrations of 4–11-fold require increases in local pH of 0.60–1.0, which do not seem unattainable given that microenvironmental effects in enzymes can change pK_a values of active site functional groups by several orders of magnitude.[14] Alternatively, the nonquantitative correspondence between apparent ΔpH and rate accelerations indicates that a microscopic pH effect may be overwhelmed by, or act independently of or synergistically with other effects such as stabilization of anionic transition states.

In addition to the $\Delta pH/\Delta pK_a$ data, spectral titrations of **2c** with **1a-d** also provided apparent dissociation constants for **1a-d**:**2c** complexes. These differed by not more than a factor of 3 from the dissociation constants determined for **1a-d**:**2b** complexes. As the spectral titrations of **2c** with **1a-d** provided more information, were simpler to carry out, and afforded more reproducible and precise results than spectral titrations of **1a-d** with **2b**, the affinity/microenvironment probe **2c** and related agents hold promise as powerful and convenient new tools for the characterization of glycopeptide–peptide interactions.

Experimental Section

General Procedure. Chemical reagents and solvents were used as received from commercial sources. ^{1}H NMR spectra were obtained at 400 MHz in Me_2SO-d_6 on a Varian XL-400 spectrometer. Chemical shifts are reported in parts per million downfield of tetramethylsilane. UV–visible spectra were recorded on a Beckman Instruments DU-7400 diode array spectrophotometer. Reverse-phase HPLC was carried out with a Beckman Instruments Model 338/167 gradient chromatography system and Rainin Dynamax 300A C18 columns. A 21.4-mm i.d. column was used for preparative separations and a 4.6-mm i.d. column was used for analytical separations. HPLC elutions employed linear gradients of 0.1% trifluoroacetic acid (TFA) in acetonitrile in 0.1% TFA in water.

Semisynthetic Vancomycin Derivatives. Vancomycin histamide (**1c**) was prepared by combining vancomycin hydrochloride (100 mg, 66 μmol) with histamine dihydrochloride (129 mg, 700 μmol), *N*-hydroxybenzotriazole (18.3 mg, 136 μmol), and triethylamine (140 mg, 138 μmol) in 2 mL of dimethyl sulfoxide (DMSO). The heterogeneous mixture was treated with dicyclohexylcarbodiimide (152 mg, 737 μmol) and stirred at room temperature for 90 h. At this time, analytical HPLC showed complete loss of vancomycin (eluted at 30% acetonitrile) and formation of a more polar major product (eluted at 28% acetonitrile). The product was purified by preparative reverse-phase HPLC and lyopholized to afford 50.3 mg (26.5 μmol, 40%) of vancomycin histamide (**1c**) ostensibly as the tris(trifluoroacetate) salt. ^{1}H NMR showed all resonances attributable to vancomycin[3] as well as new singlets at δ 8.96 and 7.38 (imidazolium C*H*s) and new triplets at δ 8.17 (amide N*H*) and 2.86 (CH_2 adjacent to the imidazolium ring). Resonances for the methylene protons adjacent to the amide were not observed; they were expected to occur at δ ~3.3, where they would have been obscured by the resonance for water. The LSIMS exhibited an ion at *m/z* 1542.5 consistent with the molecular weight calculated for the parent ion (M + H$^+$) $C_{71}H_{84}N_{12}O_{23}Cl_2$, *m/z* 1542.4. **1c** also exhibited fragment ions at *m/z* 1511.2, 1398.2, and 1236.2, which correspond to losses of CH_3NH_2, vancosamine, and vancosamine plus glucose, respectively.[4d,e]

Vancomycin propanamide (**1b**) and vancomycin 3-aminopropanamide (**1d**) were prepared using the general method outlined for **1c**. **1b** exhibited resolved diagnostic ^{1}H NMR resonances at δ 7.9 (amide N*H*), 3.07 (CH_2 adjacent to amide NH), 1.47 ($CH_2CH_2CH_3$), and 0.85 (CH_3), and an MH$^+$ ion at *m/z* 1489.4 in the LSIMS (calcd for $C_{69}H_{83}N_{10}O_{23}Cl$, *m/z* 1489.5). **1d** exhibited resolved diagnostic ^{1}H NMR resonances at δ 8.08 (amide N*H*), 2.79 (CH_2 adjacent to amine group), and 1.7 (CH_2CH_2-CH_2), and an MH$^+$ ion at *m/z* 1504.6 in the LSIMS (calcd for $C_{69}H_{84}N_{11}O_{23}Cl_2$, *m/z* 1504.5). **1b,d** also exhibited fragment ions in the LSIMS which corresponded to losses of CH_3NH_2, vancosamine, and vancosamine plus glucose.

Synthesis of Peptide Ligands and Substrates. Peptide derivatives **2a-c** were synthesized totally or in part by manual stepwise solid-phase methods using a wrist shaker and glass reaction vessels from Milligen, 9-fluorenylmethoxycarbonyl (Fmoc) amino acid derivatives from Peninsula Labs or BACHEM Bioscience, and reagents and solvents from Applied

(10) We expect that most of the rate acceleration over the uncatalyzed reaction is due to buffer-catalyzed hydrolysis.

(11) (a) Moss, R. A.; Alwis, K. W.; Bizzigotti, G. O. *J. Am. Chem. Soc.* **1983**, *105*, 681–682. (b) Menger, F. M.; Whitesell, L. G. *J. Am. Chem. Soc.* **1985**, *107*, 707–708.

(12) See, for example: Fischer, G.; Bang, H.; Berger, E.; Schellenberger, A. *Biochim. Biophys. Acta* **1984**, *791*, 87–97.

(13) Getzoff, E. D.; Cabelli, D. E.; Fisher, C. L.; Parge, H. E.; Viezzoli, M. S.; Banci, L.; Hallewell, R. A. *Nature* **1992**, *358*, 347–351.

(14) See, for example: Schmidt, D. E., Jr.; Westheimer, F. H. *Biochemistry* **1971**, *10*, 1249–1253.

Biosystems. To initiate the synthesis of each peptide, Fmoc-D-alanine was activated using dicyclohexylcarbodiimide and coupled to the solid support in dichloromethane solvent and in the presence of 0.03 equiv of 4-(dimethylamino)pyridine catalyst. Fmoc groups were removed with 20% piperidine in *N*-methylpyrrolidone (NMP). Subsequent coupling reactions were mediated by the combination of 2-(1*H*-benzotriazol-1-yl)-1,1,3,3-tetramethyluronium hexafluorophosphate (HBTU) and diisopropylethylamine in NMP.[15] Stepwise coupling efficiencies were monitored by quantitative ninhydrin analysis and were routinely >99%.[16] Additional cycles of deprotection and coupling were performed to complete each peptide. Peptides were cleaved from the solid support, purified by reverse-phase HPLC, lyopholized, and characterized by ^{1}H NMR and LSIMS.

2a was prepared using *p*-hydroxymethylphenoxymethyl (HMP) polystyrene resin from Applied Biosystems. The N-terminal acetyl group was added using 20% acetic anhydride in NMP, and the peptide was removed from the solid support using a 9:1 trifluoroacetic acid/water mixture: ^{1}H NMR δ 8.29 (d, 1H), 8.08 (d, 1H), 7.96 (d, 1H), 7.80 (t, 1H), 4.22 (m, 1H), 4.15 (m, 2H), 2.96 (m, 2H), 1.82 (s, 3H), 1.76 (s, 3H), 1.50 (m, 4H), 1.33 (m, 2H), 1.24 (d, 3H), 1.18 (d, 3H); LSIMS, for $C_{16}H_{29}N_4O_6$ (M + H$^+$), calcd *m/z* 373.2, found *m/z* 373.5.

2b was prepared using super acid sensitive resin (SASRIN) from Bachem. The *p*-nitrophenyloxycarbonyl group was attached to the N-terminus of resin-bound Gly-N^{ω}-acetyl-L-Lys-D-Ala-D-Ala by treating it with 5 equiv of *p*-nitrophenyl chloroformate in a 1:1 mixture of tetrahydrofuran and pyridine. **2b** was cleaved from the resin using 1% trifluoroacetic acid in methylene chloride: ^{1}H NMR δ 8.26 (d, 2H), 8.24 (t, 1H), 8.16 (m, 2H), 8.11 (d, 1H), 7.78 (t, 1H), 7.38 (d, 2H), 4.30 (m, 2H), 4.16 (m, 1H), 3.75 (d, 2H), 2.97 (m, 2H), 1.76 (s, 3H), 1.59 (m, 2H), 1.52 (m, 2H), 1.34 (m, 2H), 1.26 (d, 3H), 1.18 (d, 3H); LSIMS, for $C_{23}H_{33}N_6O_{10}$ (M + H$^+$), calcd *m/z* 552.2, found *m/z* 552.3.

For the preparation of **2c**, a portion of resin-bound *N*-ω-acetyl-L-Lys-D-Ala-D-Ala (an intermediate in the synthesis of **2a**) was cleaved from the solid support using a 9:1 trifluoroacetic acid/water mixture and purified by reverse-phase HPLC. A 35-mg (0.10 mmol) sample of this peptide was dissolved in 1.5 mL of DMSO and treated with 40 mg (0.10 mmol) of fluorescein isothiocyanate, isomer I (Aldrich). The reaction was stirred for 1 h at room temperature and then fractionated by reverse-phase HPLC to afford 15 mg (0.021 mmol, 21%) of **2c**: ^{1}H NMR δ 10.20 (s, 1 H), 10.12 (bs, 2H), 8.48 (d, 1H), 8.42 (s 1H), 8.19 (d, 1H), 8.12 (d, 1H), 7.79 (m, 2H), 7.17 (d, 1H), 6.67 (d, 2H), 6.55 (m, 4H), 4.92 (m, 1H), 4.35 (m, 1H), 4.20 (m, 1H), 2.95 (m, 2H), 1.76 (s, 3H), 1.73 (m, 2H), 1.39 (m, 2H), 1.3 (m, 2H), 1.27 (d, 3H), 1.22 (d, 3H); LSIMS, for $C_{35}H_{38}N_5O_{10}S$ (M + H$^+$), calcd *m/z* 720.2, found *m/z* 720.2.

Dissociation Constants. Dissociation constants for **1a-d**:**2a** complexes were determined using UV difference spectroscopy as described in the literature.[9] The titrations of **1a-d** (0.04 mM) with **2a** (0–0.1 mM) were carried out at 25 °C in 20 mM sodium citrate buffer (pH 5.1) and were monitored at 246 nm. To extract the dissociation constants, the experimental data were analyzed by nonlinear regression using the program KaleidaGraph from Synergy Software and the following expression that was derived from the simple equilibrium binding model **1** + **2a** = **1**:**2a**, K_d = [**1**][**2a**]/[**1**:**2a**]:

$$\Delta A = \frac{\Delta A_{max}}{2}\left[\left(\alpha + \frac{K_d}{[1]_0} + 1\right) - \left\{\left(\alpha + \frac{K_d}{[1]_0} + 1\right)^2 - 4\alpha\right\}^{1/2}\right] \quad (1)$$

In this equation, ΔA is the difference in absorbance at 246 nm observed upon addition of α molar equiv of **2a** to a total concentration $[1]_0$ of **1** (corrected for dilution effects and absorbance due to the peptide), and ΔA_{max} is the maximum difference in absorbance produced upon saturation of **1** with **2a**. K_d and ΔA_{max} were adjustable parameters in the analysis. The reported dissociation constants are averages of at least three independent determinations.

Kinetics. Rates of hydrolysis of **2b** were determined by monitoring increases in absorbance at 400 nm due to the appearance of the *p*-nitrophenolate anion. The experimental data were converted to the form ln(fraction **2b** remaining) versus time in order to extract the rate constants. Reactions were initiated by addition of a DMSO solution of **2b** to buffered aqueous solutions which did or did not contain catalyst. The final concentration of DMSO was 2%. For reactions catalyzed by **1a-d**, **2b** was employed in the concentration range 25–60 μM, and **1a-d** were present at 91–96 μM.

Measurement of Microscopic pH. A solution of **2c** (6.4 μM) in 20 mM sodium phosphate buffer (pH 7.0) was titrated with **1a-d** (0–20 μM), and the change in the difference in absorbance at 493 and 464 nm was monitored. The experimental data were analyzed by nonlinear regression using KaleidaGraph and the following expression that was derived from the simple equilibrium binding model **1** + **2c** = **1**:**2c**, K_d = [**1**][**2c**]/[**1**:**2c**]:

$$\Delta\Delta A = \frac{\Delta\Delta A_{max}}{2}\left[\left(\alpha + \frac{K_d}{[2c]_0} + 1\right) - \left\{\left(\alpha + \frac{K_d}{[2c]_0} + 1\right)^2 - 4\alpha\right\}^{1/2}\right] \quad (2)$$

Here, $\Delta\Delta A$ is the change in the difference in absorbance at 493 and 464 nm observed upon addition of α molar equiv of **1** to **2c**, and $\Delta\Delta A_{max}$ is the maximum change in the difference in absorbance produced upon saturation of **2c** with **1**. K_d and $\Delta\Delta A_{max}$ were adjustable parameters in the analysis. Values of $\Delta\Delta A_{max}$ were independently verified by determining $\Delta\Delta A$ after addition of 5–10 equiv of **1a-d** in powder form to a solution of **2c**. A standard curve was used to convert values of $\Delta\Delta A_{max}$ to values of ΔpH. To generate the curve, the absorption spectrum of **2c** was measured at a series of pH values between 6.0 and 8.0, and the differences in the molar extinction coefficients at 493 and 464 nm were plotted versus pH and fit to the Henderson–Hasselbalch equation:

$$pH = pK_a + \log\left[(-\Delta\epsilon_{min} + \Delta\epsilon)/(\Delta\epsilon_{max} - \Delta\epsilon)\right] \quad (3)$$

where $\Delta\epsilon_{min}$ is the minimum difference in the molar extinction coefficients, $\Delta\epsilon_{max}$ is the maximum difference in the molar extinction coefficients, and $\Delta\epsilon$ is the difference in molar extinction coefficients at a given pH. Adjustable parameters were $\Delta\epsilon_{min}$, $\Delta\epsilon_{max}$, and pK_a. This analysis provided a value of 6.50 for the pK_a of **2c**, which is equivalent to that of fluorescein. The reported ΔpH values and dissociation constants are averages of two independent determinations.

Acknowledgment. This work was supported by Stanford University, a starter grant from the NSF (CHE-9018241), a Camille and Henry Dreyfus Foundation New Faculty Award, a Shell Foundation Faculty Career Initiation Award, and a grant from the American Chemical Society Petroleum Research Fund. Vancomycin was a gift from Eli Lilly. Mass spectra were acquired by the UCSF Mass Spectrometry Facility (A.L. Burlingame, Director), supported by the Biomedical Research Technology Program of the NIH National Center for Research Resources.

(15) Fields, C. G.; Lloyd, D. H.; Macdonald, R. L.; Otteson, K. M.; Noble, R. L. *Pept. Res.* **1991**, *4*, 95–101.

(16) Sarin, V. K.; Kent, S. B. H.; Tam, J. P.; Merrifield, R. B. *Anal. Biochem.* **1981**, *117*, 147–157.